

Proceedings of “Applications of Physics in Mechanical and Material Engineering” (APMME 2023)

The Phenomenon of Magnetic Anisotropy in Amorphous Materials Produced Using the Injection-Casting Method

M. NABIAŁEK^a, J.J. WYSŁOCKI^a, T. JARUGA^b,
K. BŁOCH^a, A.V. SANDU^{c,d}, V.V. SAVINKIN^e,
M.A.A. MOHD SALLEH^{f,g} AND B. JEŻ^{b,*}

^a*Department of Physics, Faculty of Production Engineering and Materials Technology, Czestochowa University of Technology, al. Armii Krajowej 19, 42-200 Czestochowa, Poland*

^b*Department of Technology and Automation, Faculty of Mechanical Engineering and Computer Science, Czestochowa University of Technology, Al. Armii Krajowej 19c, 42-200 Czestochowa, Poland*

^c*Faculty of Material Science and Engineering, Gheorghe Asachi Technical University, 64 Dumitru Mangeron Blvd, 700050 Iasi, Romania*

^d*Academy of Romanian Scientists, 54 Splaiul Independentei St., Sect. 5, 050094 Bucharest, Romania*

^e*Department “Transport and Mechanical Engineering”, Faculty of Transport and Mechanical Engineering, M. Kozybayev North Kazakhstan University, 86 Pushkin str., 150000, Kazakhstan, Petropavlovsk*

^f*Center of Excellence Geopolymer and Green Technology, Universiti Malaysia Perlis, Taman Muhibbah, 02600 Arau, Perlis, Malaysia*

^g*Faculty of Chemical Engineering and Technology, Universiti Malaysia Perlis, Taman Muhibbah, 02600 Arau, Perlis, Malaysia*

Doi: [10.12693/APhysPolA.144.410](https://doi.org/10.12693/APhysPolA.144.410)

*e-mail: barlomiej.jez@pcz.pl

The magnetisation process of magnetic materials is extremely important due to the potential applications of these materials. During the magnetisation process, a delay in the increase in magnetisation is observed when the magnetic field strength increases. This behaviour may be explained by the magnetic anisotropy of the studied material. The paper presents the results of research on primary magnetisation curves for magnetic alloys that exhibit soft-magnetic properties. The tested alloys are the so-called amorphous materials in which determining the preferred direction of magnetisation is difficult due to their structure. However, as our research indicates, it is in fact possible to distinguish directions of relatively easy and difficult magnetisation in amorphous materials, which implies that the phenomenon of magnetic anisotropy occurs in them.

topics: magnetic anisotropy, primary magnetisation curve, saturation magnetisation, injection casting method

1. Introduction

Amorphous alloys are an interesting field of study. Due to their disordered structure, their properties differ from their crystalline counterparts with the same chemical composition [1]. Amorphous alloys are characterised by excellent mechanical properties (Ti, Zr, Fe alloys [2–4]) and/or corrosion resistance [5, 6]. Alloys with a sufficiently high proportion of ferromagnetic elements possess very good soft magnetic properties, i.e., low coercivity field value, low re-magnetisation losses and high saturation magnetisation value [7–10].

Due to the lack of an ordered structure, the domain walls can rotate quite freely, which facilitates the process of magnetisation in these materials. In crystalline materials, the magnetic structure is associated with the orientation of the crystals [11, 12]. In the case of amorphous alloys, despite the absence of an ordered structure, the easy direction of magnetisation can be determined; this is associated with the production process of these alloys [13]. So far, this phenomenon has not been fully explained, including the effect of individual alloy components on the change in anisotropy values.

The aim of this study is to investigate the effect of Cu addition on the effective anisotropy found in soft magnetic amorphous alloys based on Fe matrix.

2. Experimental procedure

The base alloy for the production of the rapidly-cooled samples was produced in an arc furnace. The ingots, each weighing 10 g, were melted and formed from high-purity ingredients: Fe, Co, Y, Cu — 99.99%, B — 99.9%. The elements were weighed with an accuracy of 0.0001 g. The mixture of elements was placed in a recess on a water-cooled copper plate. The re-melting process was carried out under a protective atmosphere of argon using a tungsten electrode. The ingots were re-melted six times physically inverting them each time in order to mix the ingredients.

Bulk, rapidly-cooled samples were produced using an injection method. The process was carried out under a protective atmosphere of argon, after having previously obtained a high vacuum in the working chamber. The base alloy was placed in a quartz crucible (with an opening of 1 mm diameter) and melted using eddy currents. The liquid alloy was forced under argon pressure into a copper mould. The samples were obtained in the form of rods, each with a length of 20 mm and a diameter of 0.5 mm.

The structure of the alloys was studied using a Bruker D8 Advance X-ray diffractometer. The diffractometer is equipped with a Cu K_α lamp. Measurements were carried out within the 2θ angle range of 30–100° on samples subjected to low-energy pulverisation.

Primary magnetisation curves and static magnetic hysteresis loops were measured using a Lake Shore 7307 vibrating sample magnetometer within the range of external magnetic field strength of up to 2 T.

3. Results

Figure 1 shows X-ray diffraction images for the investigated alloy samples. In the diffractograms, single wide maxima are visible, indicating the disordered structure of each alloy. There are no narrow peaks of significant intensity that would be associated with the presence of crystalline phases.

Figure 2 shows the static magnetic hysteresis loops measured in three directions, i.e., parallel to the casting direction, perpendicular to the casting direction, and perpendicular to the sample surface. The loops measured for the $\text{Fe}_{35}\text{Co}_{35}\text{Y}_{10}\text{B}_{20}$ alloy in the direction parallel to the casting direction and perpendicular to the casting direction are identical.

The curve measured perpendicular to the surface of the alloy (green colour) is characterised by a different shape — the alloy achieves a higher

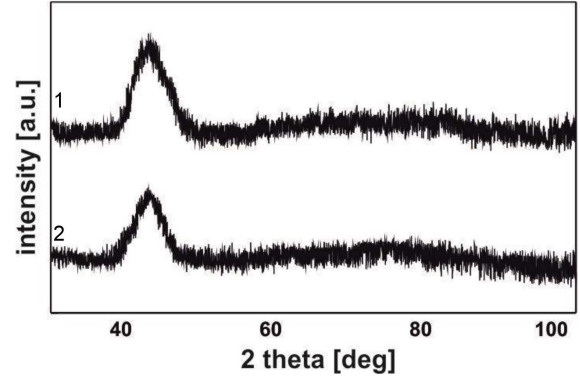


Fig. 1. X-ray diffraction patterns for the rod-form samples of the investigated alloys: curve 1 — $\text{Fe}_{35}\text{Co}_{35}\text{Y}_{10}\text{B}_{20}$, curve 2 — $(\text{Fe}_{35}\text{Co}_{35}\text{Y}_{10}\text{B}_{20})_{99}\text{Cu}_1$.

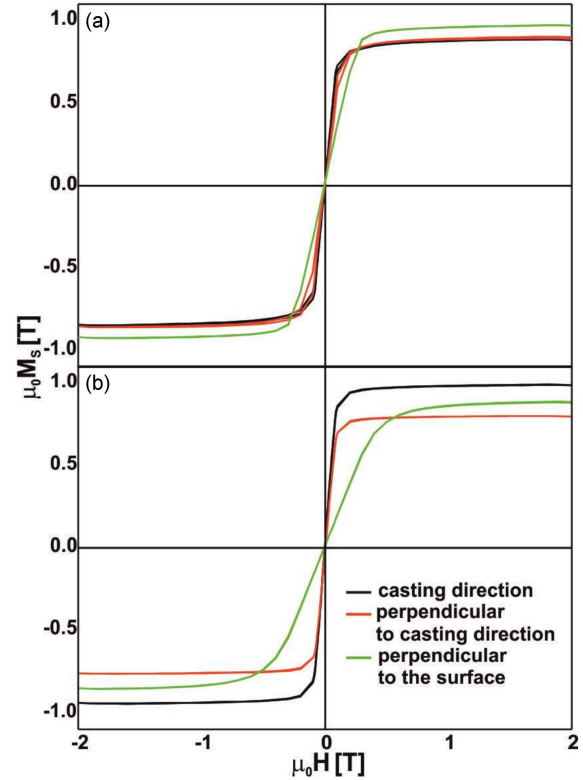


Fig. 2. Static magnetic hysteresis loops for tested amorphous alloys: (a) $\text{Fe}_{35}\text{Co}_{35}\text{Y}_{10}\text{B}_{20}$, (b) $(\text{Fe}_{35}\text{Co}_{35}\text{Y}_{10}\text{B}_{20})_{99}\text{Cu}_1$.

TABLE I

Calculated parameters: $\mu_0 M_S$ — saturation magnetisation [T], H_C — coercivity field [A/m], P_1 — anisotropy field in the first direction [kJ/m^3], P_2 — anisotropy in the second direction [kJ/m^3], P_3 — anisotropy in the third direction [kJ/m^3].

	$\mu_0 M_S$	H_C	P_1	P_2	P_3
$\text{Fe}_{35}\text{Co}_{35}\text{Y}_{10}\text{B}_{20}$	0.96	230	83	105	127
$(\text{Fe}_{35}\text{Co}_{35}\text{Y}_{10}\text{B}_{20})_{99}\text{Cu}_1$	0.95	135	55	35	207

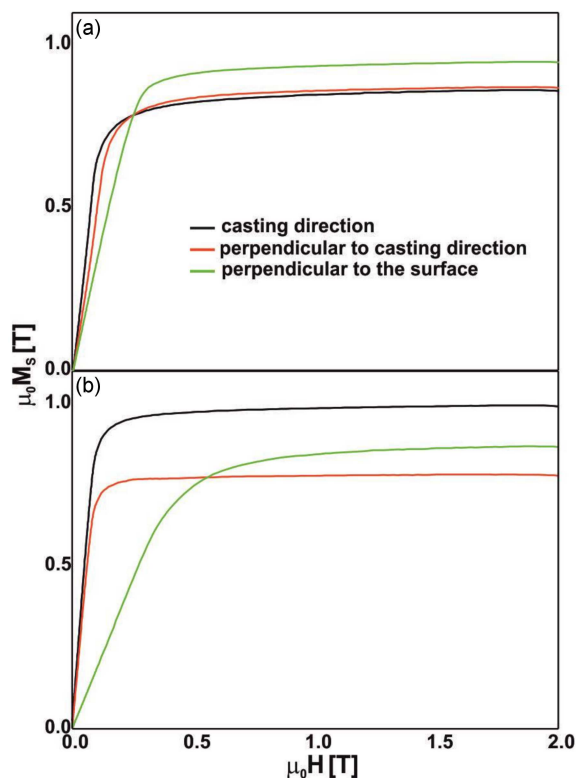


Fig. 3. Initial magnetisation curves, measured in three directions 1, 2, 3, for the tested alloys: (a) $\text{Fe}_{35}\text{Co}_{35}\text{Y}_{10}\text{B}_{20}$, (b) $(\text{Fe}_{35}\text{Co}_{35}\text{Y}_{10}\text{B}_{20})_{99}\text{Cu}_1$.

saturation of magnetisation value (M_S), but at lower values of magnetic field strength it attains a lower magnetisation value. For the alloy with the addition of Cu, similar relationships were observed, except that the curve for the perpendicular direction differs to a greater extent from the other two. The other curves (black and red) have a very similar course; however, where the sample was measured parallel to the casting direction, a much higher M_S value was achieved. The coercivity field values, measured for all three directions, reached similar values (shown in Table I).

Figure 3 shows the initial magnetisation curves, measured using the same system as the static magnetic hysteresis loops. Based on the shapes of the curves, the effective anisotropy was calculated. The results are given in Table I.

The addition of Cu causes a significant change in the shape of the primary magnetisation curves, and thus in the value of effective anisotropy. For the two easy magnetisation directions (perpendicular and parallel to the casting direction), a significant decrease in the values of P_1 and P_2 and an increase in the P_3 value were observed. In addition, the value of the coercivity field for the alloy with the addition of Cu is almost halved. Therefore, it should be assumed that the addition of Cu affects the formation of a certain short-range order in the alloy volume, and therefore the directivity in certain

areas of the alloy (it is possible that, in the volume of the alloy, there are areas similar in atomic configuration to crystalline phases). This arrangement affects the course of magnetisation, promoting it in some directions and hindering in other directions.

4. Conclusions

This paper presents the results of research on the influence of Cu on the value of effective anisotropy occurring in bulk Fe-based amorphous alloys. Based on vibrating sample magnetometer measurements, made in three different directions, it was found that easy and difficult directions of magnetisation occur in the tested alloys. In addition, a 1% addition of Cu was found to influence the degree of this effect. The alloy $(\text{Fe}_{35}\text{Co}_{35}\text{Y}_{10}\text{B}_{20})_{99}\text{Cu}_1$ is characterised by a much lower value of coercivity field and — for the easy direction of magnetisation — a much lower value of effective anisotropy.

Acknowledgments

Publication supported by IRN AP14869177 project “Development and implementation of a new high-performance mobile railway complex with resource-saving technology for laser restoration of railway wheel sets”.

References

- [1] M.E. McHenry, M.A. Willard, D.E. Laughlin, *Prog. Mater. Sci.* **44**, 291 (1999).
- [2] S. Hasani, P. Rezaei-Shahreza, A. Seifodini, *Metall. Materi. Trans. A* **50**, 63 (2019).
- [3] Y.J. Yang, B.Y. Cheng, J.W. Lv, B. Li, M.Z. Ma, X.Y. Zhang, G. Li, R.P. Liu, *Mater. Sci. Eng. A* **746**, 229 (2019).
- [4] K. Lee, S.E. Kang, *Arch. Metall. Mater.* **65**, 1357 (2020).
- [5] S. Wang, Y. Li, X. Wang, S. Yamaura, W. Zhang, *J. Non-Cryst. Solids* **476**, 75 (2017).
- [6] D.D. Liang, X.S. Wei, T.C. Ma, B. Chen, H.R. Jiang, Y. Dong, J. Shen, *J. Non-Cryst. Solids* **510**, 62 (2019).
- [7] M. Nabiątek, B. Jeż, K. Bloch, J. Gondro, K. Jeż, A.V. Sandu, P. Pietrusiewicz, *J. Alloys Compd.* **820**, 153420 (2020).
- [8] B. Jeż, J. Wysłocki, S. Walters, P. Postawa, M. Nabiątek, *Materials* **13**, 1367 (2020).
- [9] Y. Han, J. Ding, F.L. Kong, A. Inoue, S.L. Zhu, Z. Wang, E. Shalaan, F. Al-Marzouki, *J. Alloy Compd.* **691**, 364 (2017).

- [10] T. Suetsuna, H. Kinouchi, N. Sanada, *J. Magn. Magn. Mater.* **519**, 167475 (2021).
- [11] L. Zhu, S.S. Jiang, Z.Z. Yang, G.B. Han, S.S. Yan, Y.G. Wang, *J. Magn. Magn. Mater.* **519**, 167513 (2021).
- [12] S. Walters, M.M.A.B. Abdullah, A.V. Sandu, S. Garus, M.A.A. Mohd Saleh, D.S. CheHalim, F.F. Zainal, *Acta Phys. Pol. A* **139**, 568 (2021).